



Article

Dual-Band Rectifier Circuit Design for IoT Communication in 5G Systems

Ioannis D. Bougas ^{1,*}, Maria S. Papadopoulou ^{1,2}, Achilles D. Boursianis ¹, Spyridon Nikolaidis ³ and Sotirios K. Goudos ^{1,*}

¹ ELEDIA Research Center, ELEDIA@AUTH, School of Physics, Aristotle University of Thessaloniki, 54124 Thessaloniki, Greece

² Department of Information and Electronic Engineering, International Hellenic University, Alexander Campus, 57400 Sindos, Greece

³ Electronics Laboratory, School of Physics, Aristotle University of Thessaloniki, 54124 Thessaloniki, Greece

* Correspondence: impougas@physics.auth.gr (I.D.B.); sgoudo@physics.auth.gr (S.K.G.)

Abstract: Radio-frequency (RF) energy harvesting (EH) is emerging as a reliable and constantly available free energy source. The primary factor determining whether this energy can be utilized is how efficiently it can be collected. In this work, an RF EH system is presented. More particularly, we designed a dual-band RF to DC rectifier circuit at sub-6 GHz in the 5G bands, able to supply low-power sensors and microcontrollers used in agriculture, the military, or health services. The system operates at 3.5 GHz and 5 GHz in the 5G cellular network's frequency band FR1. Numerical results reveal that the system provides maximum power conversion efficiency (PCE) equal to 53% when the output load (sensor or microcontroller) is 1.74 kΩ and the input power is 12 dBm.

Keywords: Internet of Things; radio frequency energy harvesting; dual-band rectifier; wireless power transfer; impedance matching network; voltage multiplier; power conversion efficiency; 5G; voltage doubler; FR1



Citation: Bougas, I.D.; Papadopoulou, M.S.; Boursianis, A.D.; Nikolaidis, S.; Goudos, S.K. Dual-Band Rectifier Circuit Design for IoT Communication in 5G Systems. *Technologies* **2023**, *11*, 34. <https://doi.org/10.3390/technologies11020034>

Academic Editor: Ronald A. Coutu, Jr.

Received: 29 January 2023

Revised: 12 February 2023

Accepted: 21 February 2023

Published: 24 February 2023



Copyright: © 2023 by the authors. Licensee MDPI, Basel, Switzerland. This article is an open access article distributed under the terms and conditions of the Creative Commons Attribution (CC BY) license (<https://creativecommons.org/licenses/by/4.0/>).

1. Introduction

The Fourth Industrial Revolution changed the industry model by applying digitalization to old-style factories. This revolution is known as “Industry 4.0”. The 4.0 attribute focuses on the Internet of Things (IoT) applied to industrial systems [1]. The IoT is a system in which different “things”, such as people, animals, objects, computing devices, or digital machines, connect to each other and are capable of transferring data over a network without requiring any interaction between humans or humans and computers.

A “thing” in the IoT (Internet of Things) could be an animal on a farm with a biochip transponder, a human with a heart implantable device, a car that has built-in sensors to alert the driver when something goes wrong with his vehicle, or any other natural or man-made object that can take an IP (Internet Protocol) address and can transfer data via the Internet. More and more organizations in many industrial units are using the Internet of Things to work more efficiently and more professionally, to understand their customers better, enhance customer services, improve decision making, and finally increase the value of their business. Hence, nowadays, the Internet of Things is one of the most important technologies, and it will continue to grow as more and more industries and businesses understand the potential of connected devices to keep them competitive [2,3].

According to the [4,5], there is an unprecedented increase at a rate of over 50% per year of wireless data traffic for each user. This is expected to accelerate over the next 10 years with the frequent use of video and the rise of the IoT. To address this phenomenon, the wireless industry is moving towards 5G cellular technology.

With a possible peak speed of 20 Gbps and minimal latency (compared to 4G peak speed of 1 Gbps), 5G technology can enhance the performance of commercial and industrial

applications as well as other digital experiences, such as online gaming and teleconferencing. While earlier generations, such as 4G, were more concerned with providing connectivity, 5G virtualized networks take connectivity to the next level, bringing linked benefits from the cloud to clients [6].

Since the establishment of the fifth-generation (5G) cellular network, substantial new technological innovations have brought cutting-edge applications and services [7,8] to current cellular and mobile networks [9–15].

Scientists generally agree that the IoT era can significantly contribute to the current need to transition to green energy. With the evolution of electronic devices and the increase in energy requirements, the capacity to collect RF energy from dedicated or ambient sources could be used to charge low-power devices continuously and, over time, eliminate the need for batteries [16–18]. Ambient RF energy harvesting is always available as a free energy source and is omnidirectional [19]. However, its primary disadvantage is its low power. The combination of an antenna and a rectifier creates a system called a rectenna [20]. Figure 1 depicts a classic RF energy harvesting system [21] that contains a transmission antenna and a rectenna (receiving antenna, an impedance matching network (IMN), a rectifier, and a DC–DC converter). RF signals are collected from the antenna, and then the rectifier converts these signals into DC voltage. The impedance-matching network (IMN) regulates the impedance between the antenna and the rectifier. The DC–DC converter boosts and stabilizes the output of the rectifier [22].

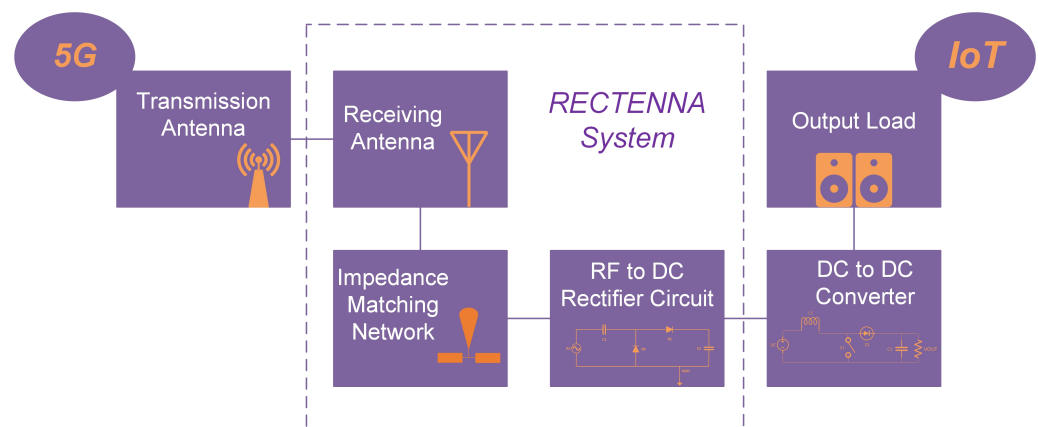


Figure 1. Complete RF energy harvesting system.

The rectifier is the most important part of the rectenna system, which significantly affects the system's efficiency [23]. The need for a rectifier circuit in autonomous systems is critical [24], especially in places with size and weight limits. There is a need for rectifiers that can transfer energy in many systems with minimum losses. In addition to that, the design of such a circuit must be very compact. There are a vast number of applications of such circuits in an IoT network. For example, in [25], there is a potential application of an IoT large-scale system that may benefit if it adopts the proposed circuit for RF energy harvesting. Additionally, other potential applications could include smart city [26], Internet of Vehicles [27,28], and Industrial IoT [29,30].

Rectennas are made to work at frequencies that are important for wireless communications and broadcast services. The fifth generation (5G) of cellular communications operates in Frequency Zone 1 (FR1), among others, at the n48, n77, and n78 bands (with a central frequency of 3.5 GHz, [31]) and the n79 band (with a central frequency of 5 GHz, [32]).

The FR1 band is defined as one of the frequency bands in which 5G technology functions [33]. The FR1 band was intended to define bands below 6 GHz, but with some additional spectrum allocations, it was extended to 7.125 GHz; hence, the FR1 zone frequencies begin from 410 MHz to 7.125 GHz. The FR2 range refers to frequencies up to 20 GHz [34,35].

In the literature, several papers present dual-band rectifiers. The main differences are in the design of the impedance-matching network and in the power conversion efficiency. In this work, we present a novel dual-band rectifier circuit for the 5G FR1 zone, and we provide a complete design framework for a low-cost RF-to-DC rectifier.

The main contribution of this paper lies in the following.

- We present a novel dual-band rectifier circuit for the 5G FR1 zone.
- We discuss and provide a complete design framework for a low-cost RF-to-DC rectifier.
- We propose a novel impedance-matching network that consists of two distinct branches, one for 3.5 GHz and the other for 5 GHz. Each branch consists of a T-shaped network with rectangular and radial stubs.
- We design a circuit design that works at 2 sub-6 GHz 5G bands, (3.5 and 5 GHz) simultaneously.

The proposed circuit achieves better power conversion efficiency than the others in the literature, as will be shown in the numerical results section. In addition to that, we have not been able to find a paper in the literature with a rectifier circuit that works at sub-6 GHz 5G bands, and only at 3.5 and 5 GHz simultaneously. This circuit can be part of an IoT node to harvest ambient RF energy, thus proving a green energy source. The IoT node may operate at a different frequency.

The remainder of this work is structured as follows: Firstly, we present the materials and methods in Section 2. In Section 3 we present the design specifications. In Section 4, we present the complete design of the proposed circuit and the numerical results. Section 5 discusses the contributions of this work and its main results. Finally, Section 6 outlines the concluding remarks of our work.

2. Materials and Methods

2.1. Related Work

RF-to-DC rectifier research can be widely categorized into integrated designs [CMOS and monolithic microwave integrated circuits (MMICs)] and discrete designs utilizing diodes or transistors. The use of CMOS technology can be found in several interesting works in the literature [36–41].

In [42], the authors fabricated a receiving antenna system that can harvest energy from Wi-Fi and WiMAX bands. This half-wave rectifier (HW) is on a Rogers RT/Duroid 5880 substrate and works at 3.5 GHz with a 0 dBm input with an efficiency of 44%. Another half-wave rectifier can be found at [43]. This rectifier achieves an efficiency of 42.5%, by using the SMS-7630 diode and having an input of -10 dBm.

Full-wave (FW) rectifiers are the best choice for achieving the best results since we can take advantage of both halves of the RF signal. In [44], the authors designed a full-wave rectifier that achieved 39.6% power conversion efficiency (PCE) at 3.8 GHz using an HSMS-2820 Schottky diode. Another full-wave rectifier was designed in [45] with a power conversion efficiency of 29.7% for an input power of 6 dBm at 3.5 GHz. At a frequency of 3.5 GHz, the authors in [46] designed a Villard voltage doubler that reaches 42% power conversion efficiency with 14 dBm input power. The authors in [47] manufactured a full-wave rectifier on Rogers RO3003 substrate with 0 dBm as input power and two Schottky diodes, SMS7630 – 079LF. They achieved a power conversion efficiency of 42% at 3.5 GHz. In [48], the authors designed a full-wave rectifier that operates at sub-6 GHz in 5G bands with a central frequency of 3.5 GHz. This rectifier achieves a maximum PCE equal to 42.5% when the output load is 1.1 k Ω and the input power reaches 9 dBm. The authors in [49] using SMS7630 diodes designed a rectifier that works at GSM900, GSM1800, UMTS2100, WiMax 3500, and Wi-Fi (2.4 and 5 GHz). They achieve 33.5% maximum PCE at -15 dBm when the frequency is 1.8 GHz. In [50], the designers fabricated a bridge rectifier that operates at 5 GHz. The circuit's conversion efficiency is up to 36.4%. A dual-band rectifier was designed in [51], which achieves 49.9% power conversion efficiency with 1.1 k Ω load resistance and 0 dBm input power at 5 GHz. The authors of [52] created a rectifier with a PCE of 51.3%, a frequency of 5.1 GHz, and an output load of 350 Ω .

2.2. Design Methodology

In our work, we demonstrate a dual-band rectifier circuit that operates in the frequency bands of the 5G cellular network, specifically at 3.5 GHz and 5 GHz. The design methodology for the rectifier circuit consists of four major steps: determining the appropriate substrate, selecting the circuit topology, selecting the appropriate diode, and designing an efficient impedance-matching network. [53]. This methodology is detailed in Figure 2 ([54]).

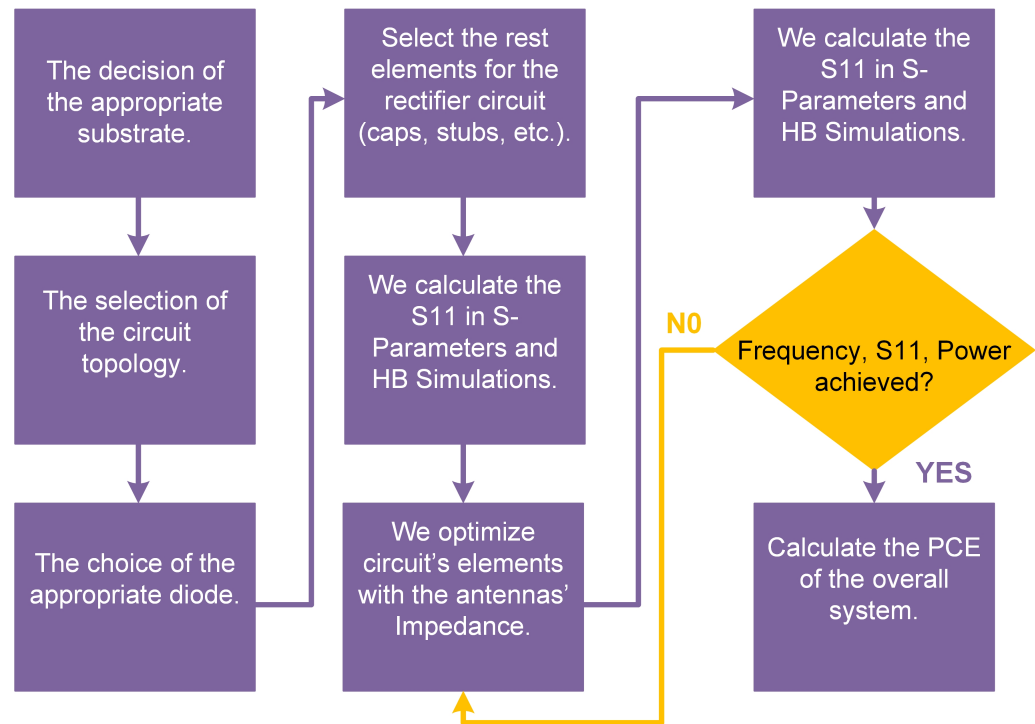


Figure 2. Design methodology.

3. Design Framework

3.1. Substrate Selection

The selection of the proper substrate is a crucial part of the design process for rectifiers. A substrate with a low dielectric constant and low dielectric loss is required. We choose the “RT/Duroid 5880” substrate, which has a copper thickness of 0.035 mm, a dielectric loss tangent of 0.0009, a thickness of 0.508 mm, and a dielectric constant of 2.2. All of these features indicate that this substrate is suitable for high-frequency applications, such as the proposed dual-band rectifier that operates at 3.5 GHz and 5 GHz [55].

3.2. Topology Selection

The voltage multiplier, the bridge of diodes, and the single diode are three basic topologies for the design of a rectifier. We designed a Greinacher voltage multiplier because this circuit not only converts the AC input to DC output but also amplifies it [56]. This topology consists of two capacitors and two Schottky diodes. Figure 3 illustrates the Greinacher topology. We see two diodes (D1, D2), two capacitors (C1, C2), an AC source, and the ground GND. In this topology, a half-wave of input sinusoidal voltage passes through one diode. Then, the opposite half-wave surges through the other. Repeating the process doubles the voltage and charges the final capacitor. As a result, the output load has a double voltage [57].

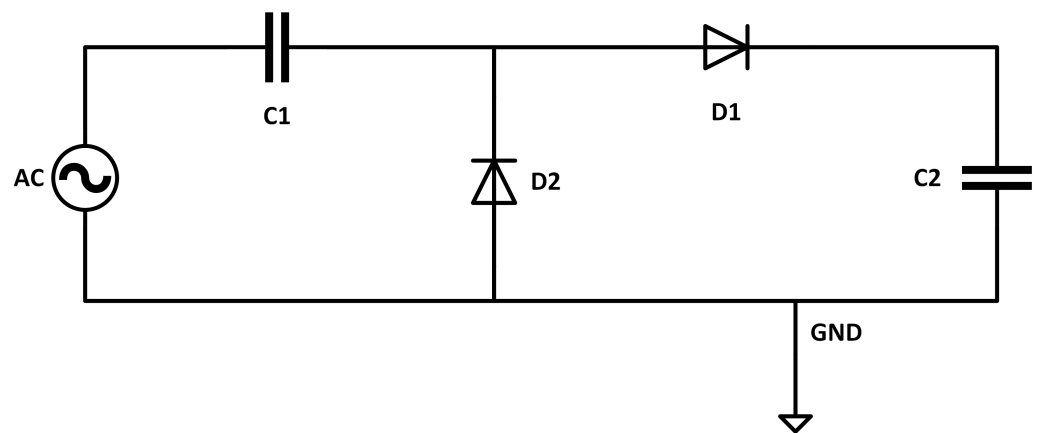


Figure 3. Greinacher topology.

3.3. Diode Selection

Diodes are a vital component in a rectifier circuit. For this circuit, we used the HSMS-286C diodes [45]. This group of diodes has been designed and optimized to work at frequencies between 915 MHz and 5.8 GHz. According to the manufacturer, these diodes are ideal for RF-to-DC conversion or voltage doubling. We achieved a high conversion efficiency thanks to their characteristics, which are the following: barrier capacitance $C_{J0} = 0.18$ pF, series resistance $R_S = 6 \Omega$, breakdown voltage $B_V = 7$ V, typical capacitance $C_T = 0.25$ pF, and $V_F = 250$ mV–350 mV [58].

3.4. Impedance-Matching Network Design

To guarantee that we have power transfer with minimum losses from the receiving antenna to the rectifier, we need to design an impedance-matching network. Thus, this circuit ensures minimum signal power reflection back to the source [59].

There are several different types of impedance-matching networks (IMNs) in the literature. These networks are made up of either distributed elements (such as microstrip lines and stubs) or lumped elements (such as inductors and capacitors). The proposed circuit works at 3.5 GHz and 5 GHz; hence, we used distributed elements because these are the best option at frequencies between 3 and 300 GHz. The lumped elements are generally used at frequencies below 3 GHz [53].

The proposed IMN consists of two distinct branches, one for 3.5 GHz and the other for 5 GHz. Each branch consists of a T-shaped network with rectangular and radial stubs. We chose radial stubs because they require less space on the chip and produce superior results. Figure 4 illustrates the appropriate impedance-matching network.

Table 1 includes the physical parameters of the transmission lines and stubs in the proposed impedance-matching network.

Table 1. Physical parameters of the transmission lines and stubs.

Parameter	Width/Length	Angle
TL1	2.7/3 mm	-
TL2	1.5/11.5 mm	-
TL3	1.5/16.6 mm	-
TL4	1/6.8 mm	-
TL5	1.5/11.5 mm	-
TL6	1.5/3 mm	-
TL7	1/15.3 mm	-
STUB1	700 nm/6.9 mm	67 degrees
STUB2	1.3/5.9 mm	33.6 degrees

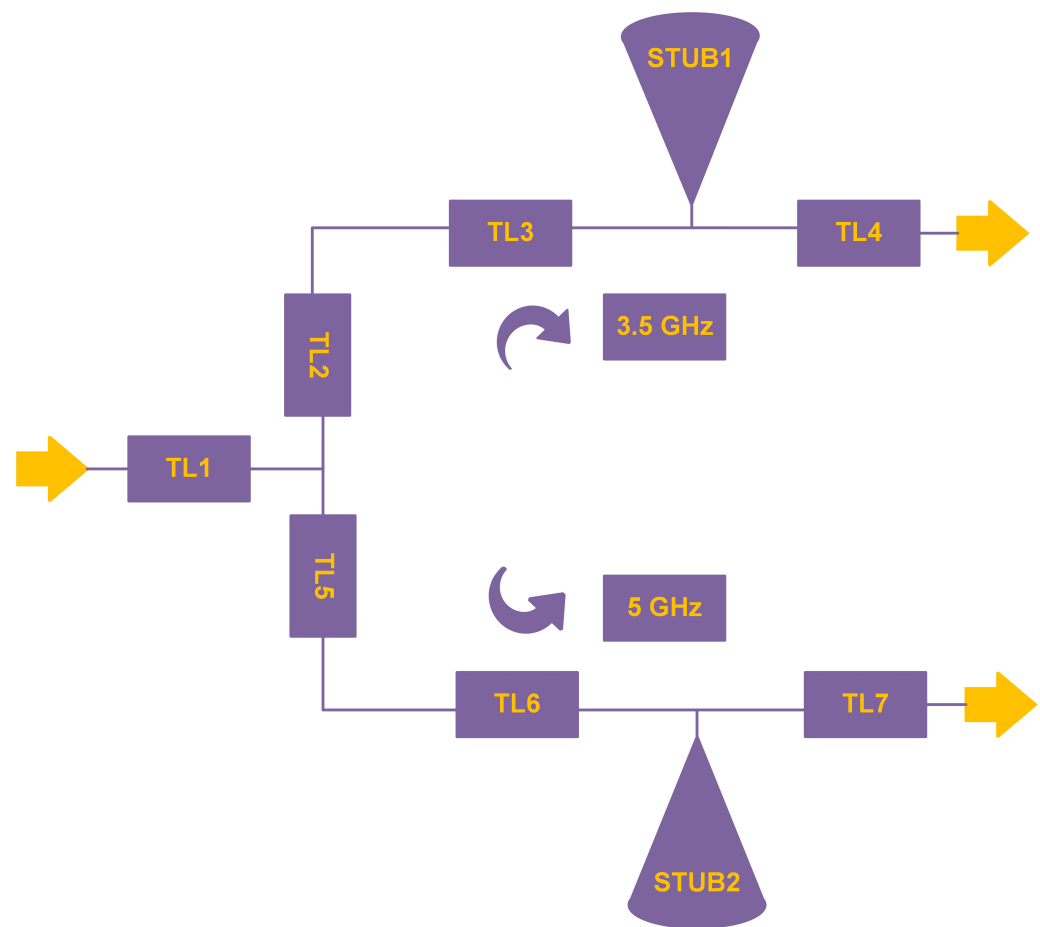


Figure 4. Proposed impedance-matching network.

4. Numerical Results

We designed a dual-band rectifier on RT/Duroid 5880. The proposed IMN is a network with two branches, one for 3.5 GHz and one for 5 GHz. As we analyzed in Section 3, each branch is a T-type network with radial and rectangular stubs. In each branch, we designed and then connected a full-wave Greinacher voltage doubler.

Each voltage doubler was built with HSMS-286C Schottky diodes and two 100pF capacitors. Furthermore, the circuit contains various conductor lines of suitable length (L) and width (W) to connect all the other components (capacitors, diodes). All of these conductor lines are the proper size to aid the impedance-matching network. The output load is connected in a differential way. As a result, we designed a differential rectifier circuit topology to produce higher output power and voltage at low input power [60].

The commercial software Advanced Design System (ADS) from Keysight Technologies, uses the gradient optimizer algorithm, which is used to design and optimize this circuit.

Figure 5 depicts the complete design of the proposed dual-band rectifier.

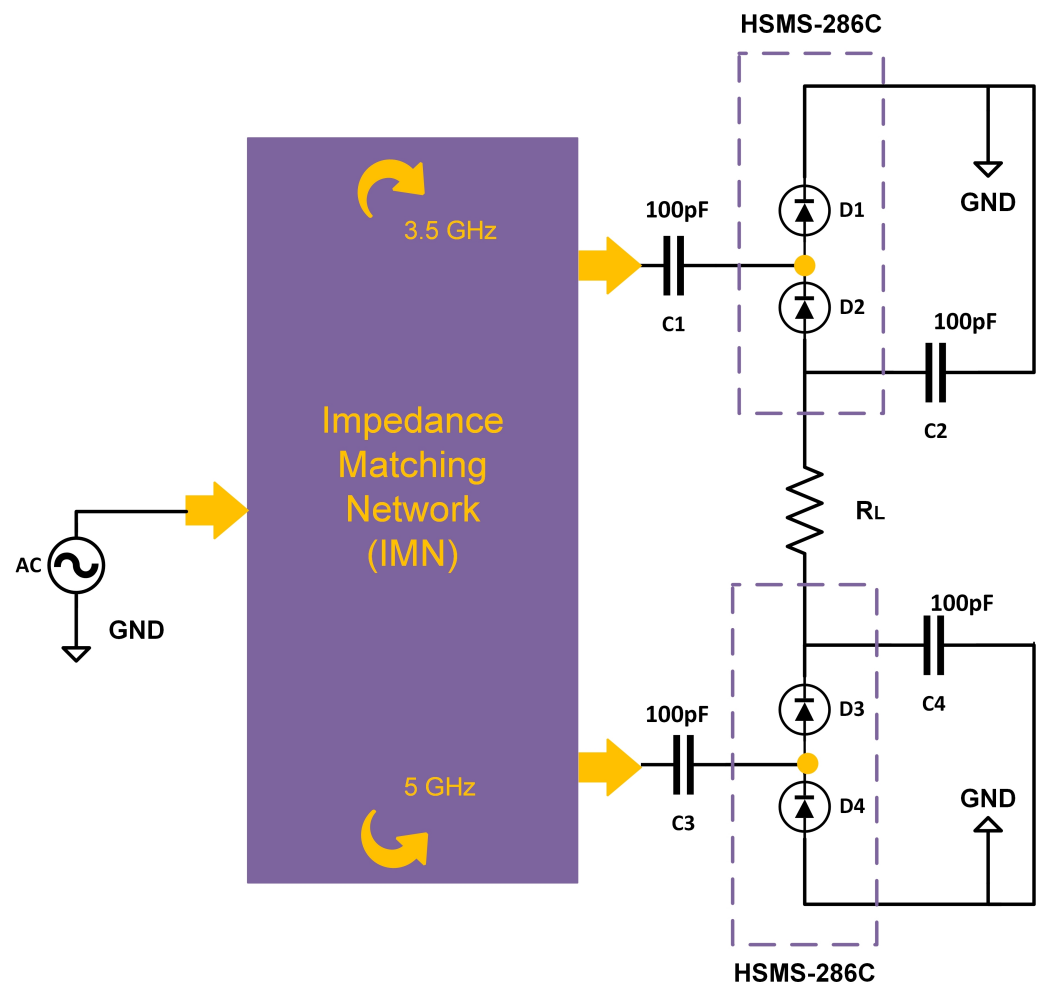


Figure 5. Proposed dual-band rectifier.

We used an antenna port of $Z_A = 50 \Omega$ as an input to design the proposed rectifier. We selected an output load with a resistance of $2 \text{ k}\Omega$. The initial impedance of the proposed circuit is $8.068 + j9.927$ at 3.5 GHz and $6.764 + j27.956$ at 5 GHz . With the design of the impedance-matching network, we want to match the impedance of the rectifier with the 50Ω impedance of the antenna. We achieved the impedance of the circuit to be $50.057 - j0.161$ at 3.5 GHz and $49.921 - j0.267$ at 5 GHz by implementing the IMN, which we analyzed in the previous section. Figure 6 illustrates the reflection coefficient frequency response. The S_{11} value at 3.5 GHz and 5.0 GHz design frequencies is -55.335 dB and -51.114 dB , respectively. Furthermore, as shown in Figure 6, the $S_{11} < -10 \text{ dB}$ impedance matching this dual-band rectifier is equal to 80 MHz at 3.5 GHz and 90 MHz at 5 GHz . We note that the proposed circuit performs well in all the above cases.

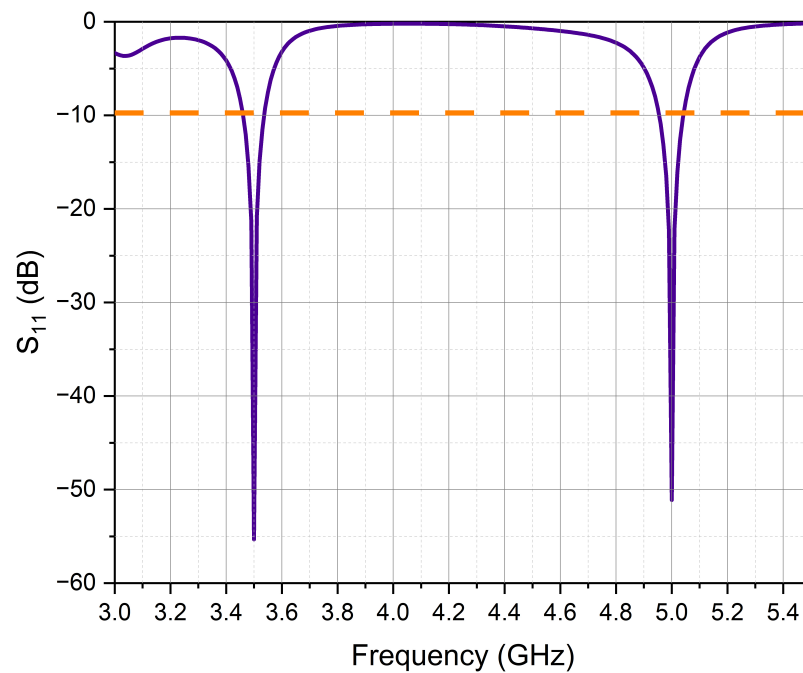


Figure 6. S_{11} Reflection coefficient.

One of the most noteworthy parts of the design is the output load. The choice of the output load determines the total RF-to-DC efficiency $n\%$ of the circuit. Equation (1), shows that when the output load increases, the efficiency of the circuit decreases. The total RF-to-DC efficiency $n\%$ is computed as follows:

$$n = \frac{P_{in}}{P_{out}}, P_{out} = \frac{V_{out}^2}{R_L}, \quad (1)$$

we classify the RF input power P_{in} , the output power P_{out} , the output voltage V_{out} , and the output load R_L .

Since we want to maximize the efficiency $n\%$, we set a harmonic balance (HB) simulation to see the values of R_L and P_{in} , thus having better power conversion efficiency $n\%$. Figure 7 displays the power conversion efficiency versus the output load R_L of the proposed rectifier circuit. In this graph, we observe that the initial design has an output load of 2 k Ω and an input power of 12 dBm and achieves PCE 52.4%. Moreover, we can easily derive that the maximum power conversion efficiency of the proposed circuit is 53% for an input power of 12 dBm and output load value of 1.74 k Ω . In addition, the proposed dual-band rectifier works well enough for low input power. The circuit achieves PCE, 22.5% for input power -6 dBm and output load of 3.4 k Ω , 32.1% for input power -3 dBm and output load of 3.4 k Ω , 40% for input power 0 dBm and output load of 3.16 k Ω and 49.5% for input power 3 dBm and output load of 2.32 k Ω .

Figure 8 displays the power conversion efficiency versus the input power P_{in} for the 3.5 GHz and 5 GHz bands separately. In this graph, we observe that the proposed rectifier has an output load of 1.74 k Ω achieves in 12 dBm PCE 22.7% at 3.5 GHz and 30.7% at 5 GHz.

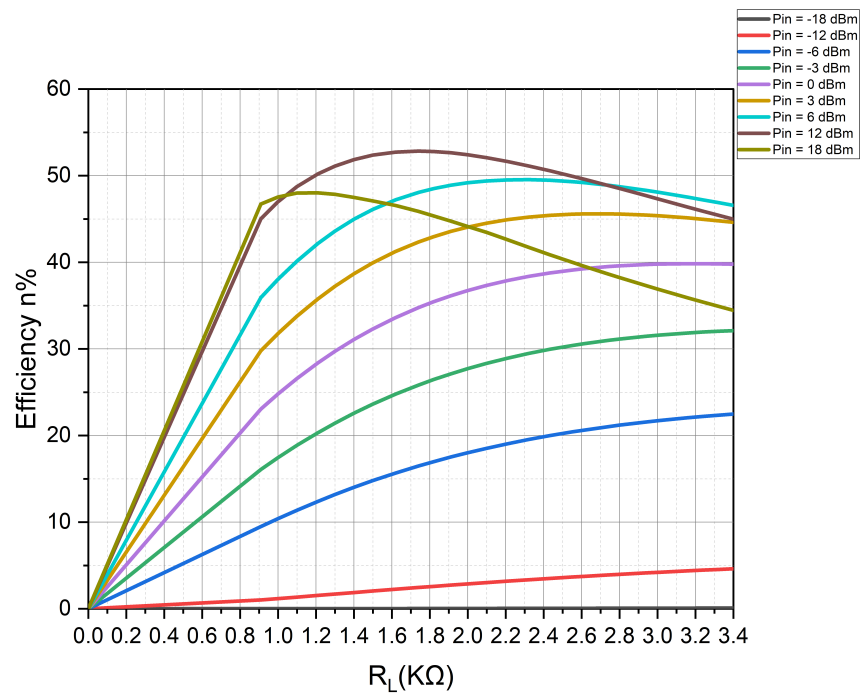


Figure 7. Power conversion efficiency versus the output load R_L .

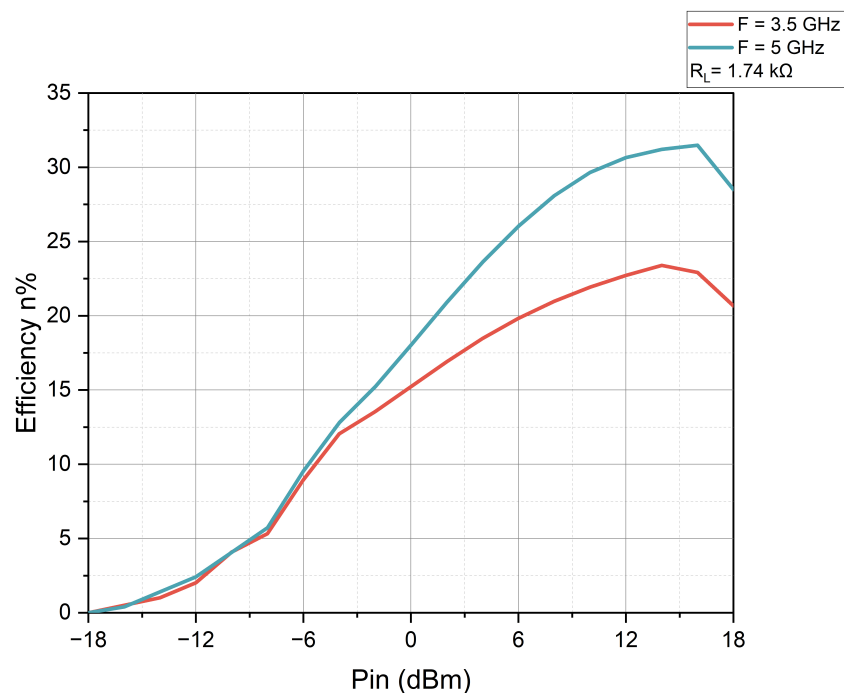


Figure 8. Power conversion efficiency versus input power P_{in} .

In addition to output power, the output voltage is an important value. Figure 9 displays the output voltage of the rectifier versus the input power for an output load of $2\text{ k}\Omega$. We observe that we have a greater output voltage for 18 dBm input power, but for low input voltage (such as 0 dBm), we have remarkable output voltages. When we have maximum power conversion efficiency, the output voltage is equal to 3.8 V , while it is equal to 7.5 V when the output load is $2\text{ k}\Omega$ and the input power is 18 dBm (Figure 9). As can be expected, as the input power increases, so does the output voltage.

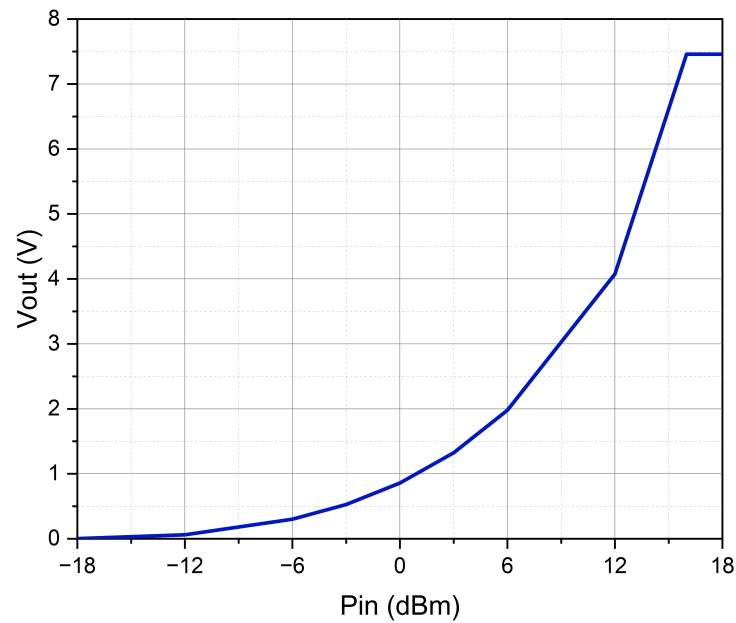


Figure 9. Output voltage versus input power.

Figure 10 below illustrates the layout of our dual-band rectifier circuit.

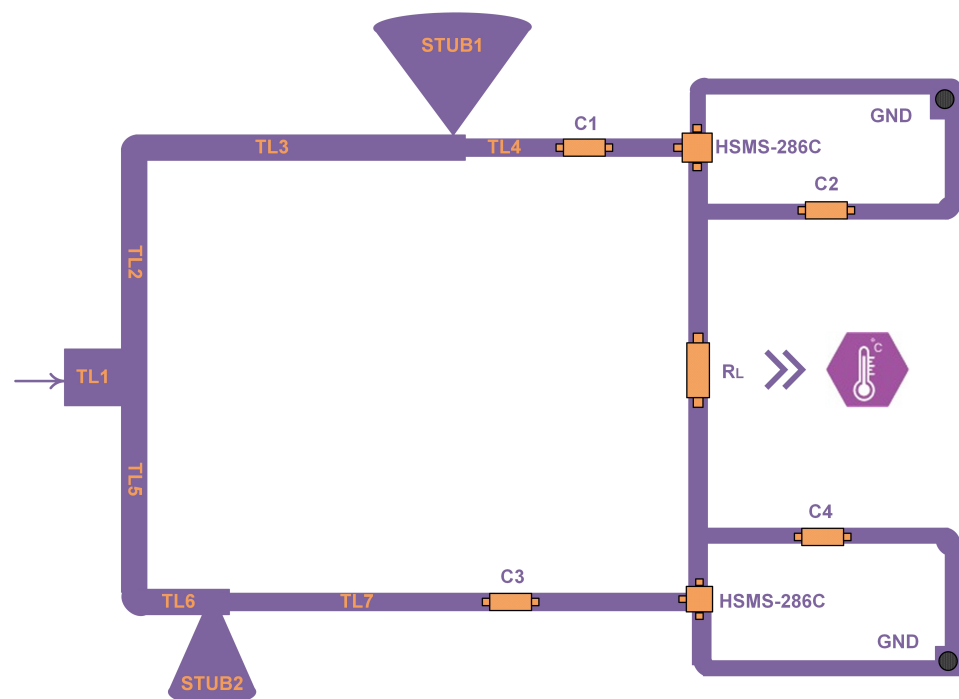


Figure 10. Layout of the proposed rectifier.

Table 2 compares the proposed rectifier to previous works that are full- and half-wave rectifiers operating at frequencies of 3.5 and 5 GHz, respectively. It is remarkable that among the designs, the proposed circuit design is the only one that works at sub-6 GHz 5G bands and only at 3.5 and 5 GHz simultaneously.

Table 2. Comparative results between proposed dual-band rectifier and previous works.

Reference	Type of Circuit	Substrate	Diode	Frequency (GHz)	P_{in} (dBm)	R_L (k Ω)	PCE (%) @ Desired Frequencies	V_{out}
[42]	Half-Wave rectifier	RT/Duroid 5880	SMS-7630	3.5, 5.8	0	0.5	44	656.88 mV
[43]	Half-Wave rectifier	FR-4	SMS-7630	2.4, 3.5	−10	-	42.5	-
[44]	Full-Wave rectifier	FR-4	HSMS-2820	2.45, 3.8	20	0.230	39.6	4.23 V
[45]	Full-Wave rectifier	FR-4	HSMS-2860	3.5	6	1	29.7	0.82 V
[46]	Full-Wave rectifier	FR-4	HSMS-286C	1.9, 2.5, 3.6	14	3	42	5.53 V
[47]	Full-Wave rectifier	Rogers RO3003	SMS-7630 – 079 LF	3.51	0	2	42	-
[48]	Full-Wave rectifier	RT/Duroid 5880	HSMS-286C	3.5	9	1.1	42.5	-
[49]	Full-Wave rectifier	-	SMS-7630	0.9, 1.8, 2.1, 2.4, 5	−15	-	33.5 (@ 1.8 GHz)	0.5 V
[50]	Full-Wave rectifier	-	Gallium Arsenide printed diodes	5	-	-	36.4	-
[51]	Full-Wave rectifier	FR-4	HSMS-286B	2.45, 5	0	1.1	49.9	0.236 V
[52]	Full-Wave rectifier	-	-	5.1	15	0.350	51.3	-
This Work	Full-Wave rectifier	RT/Duroid 5880	HSMS-286C	3.5, 5	12	1.74	53	3.815 V

5. Discussion

The Fourth Industrial Revolution improved the industry model by applying digitalization to traditional industrial units. This revolution is known as “Industry 4.0.” The 4.0 attribute focuses on the Internet of Things (IoT) applied to industrial systems.

There is an increase of over 50% per year in wireless data traffic for each user. This is estimated to accelerate over the next few years with the frequent use of video and the growth of the IoT. The wireless industry is moving to 5G cellular technology to address this phenomenon.

The technological innovations the Internet of Things (IoT) brings have led to more green energy sources. IoT is a system that can transfer data over a network without requiring interaction between humans or humans and computers. One example of a green source is radio-frequency (RF) which is omnidirectional and always available.

The growth of 5G has led to substantial technological innovations and the development of cutting-edge applications and services. In Frequency Zone 1 (FR1), 5G operates, among others, at the n48, n77, n78, and n79 bands.

In this work, we have presented a novel dual-band rectifier circuit (discrete design) that works at frequencies of 3.5 and 5 GHz. The design methodology of this rectifier has four steps: the decision for the appropriate substrate, the selection of the circuit topology, the choice of the appropriate diode, and the design of an effective impedance-matching network. For this circuit, we need a substrate with a low dielectric constant and low dielectric loss; hence, we selected the “RT/Duroid 5880” substrate. Then, we designed a Greinacher voltage multiplier. In addition, for this circuit, we used the HSMS-286C diodes. To guarantee that we have a power transfer with minimum losses from the receiving

antenna to the rectifier, we designed an impedance-matching network with distributed elements.

After finalizing the design, the S_{11} value is -55.335 dB and -51.114 dB at frequencies of 3.5 and 5 GHz, respectively. Furthermore, the $S_{11} -10$ dB bandwidth (BW) is 80 MHz at 3.5 GHz and 90 MHz at 5 GHz. With an input power of 12 dBm and an output load of 2 k Ω , we achieved a PCE of 52.4% and an output voltage of 4.074 V. Lastly, this full-wave rectifier performed exceptionally well with low input power.

It is notable that among the designs, the proposed circuit design is the only one that works at sub-6 GHz 5G bands and only at 3.5 and 5 GHz simultaneously. Additionally, this design can be used in several technological fields, such as military services, therapeutic, or telecommunication services. It can also be useful for different IoT applications that require energy harvesting.

Energy harvesting is undeniably an excellent technique for numerous self-powered microsystems. Mobile phones, wireless sensors, remote weather stations, calculators, watches, and Bluetooth are additional examples of such systems. Numerous companies have introduced mobile phones that charge using radio frequency (RF) signals. With the rapid growth of the IoT in recent years, RF energy harvesting will play a crucial role due to the limitless nature of RF signals. Rectenna systems will be of great use in smart homes and smart cities, which are also significant new scientific fields. It aims to solve the power supply issue of the innumerable IoT sensors, thereby contributing to the need to reduce their power supply or battery. It is not necessary to restrict energy harvesting to RF signals because there are numerous other sources, such as kinetic, chemical, friction, heat radiation, solar, etc. Consequently, the future of energy harvesting may involve combining these forms of energy to increase energy efficiency.

Regarding our future work, we intend to improve the PCE and the output voltage of the rectifier circuit. Moreover, we plan to make the rectifier operate at more frequencies. For example, we would like to make a rectifier that works at additional frequency bands such as 2.4 GHz and 6 GHz. In addition to that, we will try to improve the voltage and power efficiency of the total circuit.

6. Conclusions

In this work, we proposed a dual-band RF to DC rectifier at sub-6 GHz 5G bands. The circuit was designed on an RT/Duroid 5880 substrate with a dielectric constant of 2.2. This circuit is suitable to work within Frequency Zone 1 (FR1) in the n48, n77, and n78 bands with a central frequency of 3.5 GHz and the n79 with a central frequency of 5 GHz. The Avago HSMS-286C diodes were utilized, while the Greinacher topology was selected. The impedance-matching network has distributed elements that consist of two different branches, one for 3.5 GHz and one for 5 GHz. The system presents a PCE of 53% when the output load is 1.74 k Ω and the input power is 12 dBm. The output DC voltage is 3.8 V, and it can supply low-power electronic devices, such as sensors and microcontrollers.

Author Contributions: Conceptualization, I.D.B. and M.S.P.; methodology, I.D.B., M.S.P. and A.D.B.; software, I.D.B., M.S.P. and A.D.B.; validation, I.D.B., M.S.P. and A.D.B.; formal analysis, I.D.B., M.S.P. and A.D.B.; investigation, S.N.; resources, S.N.; data curation, S.K.G.; writing—original draft preparation, I.D.B.; writing—review and editing, S.K.G.; visualization, I.D.B., M.S.P. and A.D.B.; supervision, S.K.G. and S.N.; project administration, S.K.G. All authors have read and agreed to the published version of the manuscript.

Funding: This research received no external funding.

Data Availability Statement: Data sharing not applicable.

Conflicts of Interest: The authors declare no conflict of interest.

References

1. Roda-Sanchez, L.; Garrido-Hidalgo, C.; Hortelano, D.; Olivares, T.; Ruiz, M.C. OperABLE: An IoT-based wearable to improve efficiency and smart worker care services in Industry 4.0. *J. Sens.* **2018**, *2018*, 6272793. [[CrossRef](#)]
2. Boursianis, A.D.; Papadopoulou, M.S.; Damantoulakis, P.; Karampatea, A.; Doanis, P.; Geourgoulas, D.; Skoufa, A.; Valavanis, D.; Apostolidis, C.; Babas, D.G.; et al. Advancing Rational Exploitation of Water Irrigation Using 5G-IoT Capabilities: The AREThOU5A Project. In Proceedings of the 2019 29th International Symposium on Power and Timing Modeling, Optimization and Simulation (PATMOS), Rhodes, Greece, 1–3 July 2019; pp. 127–132. [[CrossRef](#)]
3. What is the Internet of Things (IoT)? 2022. Available online: <https://www.techtarget.com/iotagenda/definition/Internet-of-Things-IoT> (accessed on 14 September 2022).
4. Rappaport, T.S.; Xing, Y.; MacCartney, G.R.; Molisch, A.F.; Mellios, E.; Zhang, J. Overview of Millimeter Wave Communications for Fifth-Generation (5G) Wireless Networks—With a Focus on Propagation Models. *IEEE Trans. Antennas Propag.* **2017**, *65*, 6213–6230. [[CrossRef](#)]
5. Tseliou, G.; Adelantado, F.; Verikoukis, C. A Base Station Agnostic Network Slicing Framework for 5G. *IEEE Netw.* **2019**, *33*, 82–88. [[CrossRef](#)]
6. What Is 5G? Available online: <https://www.cisco.com/c/en/us/solutions/what-is-5g.html> (accessed on 31 January 2023).
7. Song, C.; Ding, Y.; Eid, A.; Hester, J.G.D.; He, X.; Bahr, R.; Georgiadis, A.; Goussetis, G.; Tentzeris, M.M. Advances in Wirelessly Powered Backscatter Communications: From Antenna/RF Circuitry Design to Printed Flexible Electronics. *Proc. IEEE* **2022**, *110*, 171–192. [[CrossRef](#)]
8. Daskalakis, S.N.; Georgiadis, A.; Tentzeris, M.M.; Goussetis, G.; Deligeorgis, G. The New Era of Long-Range “Zero-Interception” Ambient Backscattering Systems: 130 m with 130 nA Front-End Consumption. *Sensors* **2022**, *22*, 4151. [[CrossRef](#)]
9. Costa, C.M.d.; Baltus, P. Design Methodology for Industrial Internet-of-Things Wireless Systems. *IEEE Sens. J.* **2021**, *21*, 5529–5542. [[CrossRef](#)]
10. Pliatsios, D.; Sarigiannidis, P.; Goudos, S.; Karagiannidis, G.K. Realizing 5G vision through Cloud RAN: Technologies, challenges, and trends. *EURASIP J. Wirel. Commun. Netw.* **2018**, *2018*, 1–15. [[CrossRef](#)]
11. Rappaport, T.S.; Sun, S.; Mayzus, R.; Zhao, H.; Azar, Y.; Wang, K.; Wong, G.N.; Schulz, J.K.; Samimi, M.; Gutierrez, F. Millimeter Wave Mobile Communications for 5G Cellular: It Will Work! *IEEE Access* **2013**, *1*, 335–349. [[CrossRef](#)]
12. Esteves, V.; Antonopoulos, A.; Kartsakli, E.; Puig-Vidal, M.; Miribel-Català, P.; Verikoukis, C. Cooperative Energy Harvesting-Adaptive MAC Protocol for WBANs. *Sensors* **2015**, *15*, 12635–12650. [[CrossRef](#)]
13. Rangan, S.; Rappaport, T.S.; Erkip, E. Millimeter-Wave Cellular Wireless Networks: Potentials and Challenges. *Proc. IEEE* **2014**, *102*, 366–385. [[CrossRef](#)]
14. Mekikis, P.V.; Lalos, A.S.; Antonopoulos, A.; Alonso, L.; Verikoukis, C. Wireless Energy Harvesting in Two-Way Network Coded Cooperative Communications: A Stochastic Approach for Large Scale Networks. *IEEE Commun. Lett.* **2014**, *18*, 1011–1014. [[CrossRef](#)]
15. Palazzi, V.; Correia, R.; Gu, X.; Hemour, S.; Wu, K.; Costanzo, A.; Masotti, D.; Fazzini, E.; Georgiadis, A.; Kazemi, H.; et al. Radiative Wireless Power Transfer: Where We Are and Where We Want to Go. *IEEE Microw. Mag.* **2023**, *24*, 57–79. [[CrossRef](#)]
16. Bi, S.; Ho, C.K.; Zhang, R. Wireless powered communication: Opportunities and challenges. *IEEE Commun. Mag.* **2015**, *53*, 117–125. [[CrossRef](#)]
17. Parzysz, F.; Ntontin, K.; Kalaboukas, K.; Verikoukis, C. Dedicated RF Power Transfer for Wirelessly-Powered Wearable Medical Sensors. In Proceedings of the 2016 IEEE Global Communications Conference (GLOBECOM), Washington, DC, USA, 4–8 December 2016; pp. 1–6. [[CrossRef](#)]
18. Otal, B.; Alonso, L.; Verikoukis, C. Energy-efficiency analysis of a distributed queuing medium access control protocol for biomedical wireless sensor networks in saturation conditions. *Sensors* **2011**, *11*, 1277–1296. [[CrossRef](#)]
19. Mirzababae, N.; Geran, F.; Mohanna, S. A radio frequency energy harvesting rectenna for GSM, LTE, WLAN, and WiMAX. *Int. J. RF Microw. Comput.-Aided Eng.* **2021**, *31*, e22630. [[CrossRef](#)]
20. Brown, W.C. The history of power transmission by radio waves. *IEEE Trans. Microw. Theory Tech.* **1984**, *32*, 1230–1242. [[CrossRef](#)]
21. Mishra, D.; De, S.; Jana, S.; Basagni, S.; Chowdhury, K.; Heinzelman, W. Smart RF energy harvesting communications: Challenges and opportunities. *IEEE Commun. Mag.* **2015**, *53*, 70–78. [[CrossRef](#)]
22. Forouzes, M.; Siwakoti, Y.P.; Gorji, S.A.; Blaabjerg, F.; Lehman, B. Step-Up DC–DC Converters: A Comprehensive Review of Voltage-Boosting Techniques, Topologies, and Applications. *IEEE Trans. Power Electron.* **2017**, *32*, 9143–9178. [[CrossRef](#)]
23. Ibrahim, H.H.; Singh, M.J.; Al-Bawri, S.S.; Ibrahim, S.K.; Islam, M.T.; Alzamil, A.; Islam, M.S. Radio frequency energy harvesting technologies: A comprehensive review on designing, methodologies, and potential applications. *Sensors* **2022**, *22*, 4144. [[CrossRef](#)]
24. Belleville, M.; Cantatore, E.; Fanet, H.; Fiorini, P.; Nicole, P.; Pelgrom, M.; Pigué, C.; Hahn, R.; Van Hoof, C.; Vullers, R.; et al. *Energy Autonomous Systems: Future Trends in Devices, Technology, and Systems*; CATRENE: Paris, France, 2009.
25. De Vito, L.; Cocca, V.; Riccio, M.; Tudosa, I. Wireless Active Guardrail System for environmental measurements. In Proceedings of the 2012 IEEE Workshop on Environmental Energy and Structural Monitoring Systems (EESMS), Perugia, Italy, 28 September 2012; pp. 50–57. [[CrossRef](#)]
26. Chen, C.; Jiang, J.; Zhou, Y.; Lv, N.; Liang, X.; Wan, S. An edge intelligence empowered flooding process prediction using Internet of things in smart city. *J. Parallel Distrib. Comput.* **2022**, *165*, 66–78. [[CrossRef](#)]

27. Chen, C.; Li, H.; Li, H.; Fu, R.; Liu, Y.; Wan, S. Efficiency and Fairness Oriented Dynamic Task Offloading in Internet of Vehicles. *IEEE Trans. Green Commun. Netw.* **2022**, *6*, 1481–1493. [CrossRef]
28. Liu, S.; Yu, J.; Deng, X.; Wan, S. FedCPF: An Efficient-Communication Federated Learning Approach for Vehicular Edge Computing in 6G Communication Networks. *IEEE Trans. Intell. Transp. Syst.* **2022**, *23*, 1616–1629. [CrossRef]
29. Lu, J.; Liu, H.; Zhang, Z.; Wang, J.; Goudos, S.; Wan, S. Toward Fairness-Aware Time-Sensitive Asynchronous Federated Learning for Critical Energy Infrastructure. *IEEE Trans. Ind. Inform.* **2022**, *18*, 3462–3472. [CrossRef]
30. Lu, J.; Liu, H.; Jia, R.; Wang, J.; Sun, L.; Wan, S. Towards Personalized Federated Learning Via Group Collaboration in IIoT. *IEEE Trans. Ind. Inform.* **2022**, 1–10. [CrossRef]
31. 3GPP: 5G-NR Specifications Series. Available online: <https://www.3gpp.org/dynareport?code=38-series.htm> (accessed on 14 September 2022).
32. 5G Frequency Bands & Spectrum Allocations. 2021. Available online: <https://www.cablefree.net/wirelesstechnology/4glte/5g-frequency-bands-lte/> (accessed on 14 September 2022).
33. 5G FR1 Frequency Bands. 2021. Available online: <https://www.everythingrf.com/community/5g-fr1-frequency-bands> (accessed on 14 September 2022).
34. Dilli, R. Analysis of 5G Wireless Systems in FR1 and FR2 Frequency Bands. In Proceedings of the 2020 2nd International Conference on Innovative Mechanisms for Industry Applications (ICIMIA), Bangalore, India, 5–7 March 2020; pp. 767–772. [CrossRef]
35. 5G Frequency Bands, Channels for FR1 & FR2. 2021. Available online: <https://www.electronics-notes.com/articles/connectivity/5g-mobile-wireless-cellular/frequency-bands-channels-fr1-fr2.php> (accessed on 14 September 2022).
36. Dehghani, S.; Johnson, T. A 2.4-GHz CMOS Class-E Synchronous Rectifier. *IEEE Trans. Microw. Theory Tech.* **2016**, *64*, 1655–1666. [CrossRef]
37. Chatterjee, S.; Tarique, M. A 100-nW Sensitive RF-to-DC CMOS Rectifier for Energy Harvesting Applications. In Proceedings of the 2016 29th International Conference on VLSI Design and 2016 15th International Conference on Embedded Systems (VLSID), Kolkata, India, 4–8 January 2016; pp. 557–558. [CrossRef]
38. Jantarachote, V.; Tontisirin, S.; Akkaraekthalin, P.; Negra, R.; Chalermwisutkul, S. CMOS rectifier design for RFID chip with high sensitivity at low input power to be combined with an ultrasmall antenna. *Int. J. Numer. Model. Electron. Netw. Devices Fields* **2019**, *32*, e2607. [CrossRef]
39. Rosli, M.; Murad, S.; Norizan, M.; Ramli, M. Design of RF to DC conversion circuit for energy harvesting in CMOS 0.13- μ m technology. *AIP Conf. Proc.* **2018**, *2045*, 0200892018. [CrossRef]
40. Lo, Y.L.; Chuang, Y.H. A High-Efficiency CMOS Rectifier with Wide Harvesting Range and Wide Band Based on MPPT Technique for Low-Power IoT System Applications. *Circuits Syst. Signal Process.* **2017**, *36*, 5019–5040. [CrossRef]
41. Basim, M.; Khan, D.; Ain, Q.U.; Shehzad, K.; Shah, S.A.A.; Jang, B.G.; Pu, Y.G.; Yoo, J.M.; Kim, J.T.; Lee, K.Y. A Highly Efficient RF-DC Converter for Energy Harvesting Applications Using a Threshold Voltage Cancellation Scheme. *Sensors* **2022**, *22*, 2659. [CrossRef]
42. Derbal, M.C.; Nedil, M. A high gain dual band rectenna for RF energy harvesting applications. *Prog. Electromagn. Res. Lett.* **2020**, *90*, 29–36. [CrossRef]
43. Eltresy, N.; Eisheakh, D.; Abdallah, E.; Elhenawy, H. RF Energy Harvesting Using Efficiency Dual Band Rectifier. In Proceedings of the 2018 Asia-Pacific Microwave Conference (APMC), Kyoto, Japan, 6–9 November 2018; pp. 1453–1455. [CrossRef]
44. Zied, C.M.; Rashid, E.R.; Hareb, A. Harvesting microwave energy from WiMax bands based on a Dual-Band Antenna. *IOP Conf. Ser. Earth Environ. Sci.* **2019**, *227*, 042044. [CrossRef]
45. Dardeer, O.M.A.; Elsadek, H.A.; Abdallah, E.A. Compact Broadband Rectenna for Harvesting RF Energy in WLAN and WiMAX Applications. In Proceedings of the 2019 International Conference on Innovative Trends in Computer Engineering (ITCE), Aswan, Egypt, 2–4 February 2019; pp. 292–296. [CrossRef]
46. Sarma, S.S.; Chandravanshi, S.; Akhtar, M.J. Triple band differential rectifier for RF energy harvesting applications. In Proceedings of the 2016 Asia-Pacific Microwave Conference (APMC), New Delhi, India, 5–9 December 2016; pp. 1–4. [CrossRef]
47. Azam, S.K.; Islam, M.S.; Hossain, A.Z.; Othman, M. Monopole antenna on transparent substrate and rectifier for energy harvesting applications in 5G. *Int. J. Adv. Comput. Sci. Appl.* **2020**, *11*, 84–89. [CrossRef]
48. Bougas, I.D.; Papadopoulou, M.S.; Boursianis, A.D.; Sarigiannidis, P.; Nikolaidis, S.; Goudos, S.K. Rectifier circuit design for 5G energy harvesting applications. In Proceedings of the 2022 11th International Conference on Modern Circuits and Systems Technologies (MOCASST), Samos, Greece, 3–7 July 2022; pp. 1–4. [CrossRef]
49. Usman, M.; Khan, W.T. Six Band RF Energy Harvesting From Ambient Signals. 2019. Available online: https://www.mtt.org/app/uploads/2019/01/10-Final-Report_Usman.pdf (accessed on 14 September 2022).
50. Jung, Y.H.; Zhang, H.; Lee, I.K.; Shin, J.H.; Kim, T.i.; Ma, Z. Releasable high-performance GaAs Schottky diodes for gigahertz operation of flexible bridge rectifier. *Adv. Electron. Mater.* **2019**, *5*, 1800772. [CrossRef]
51. Mohd Noor, F.S.; Zakaria, Z.; Lago, H.; Meor Said, M.A. Dual-band aperture-coupled rectenna for radio frequency energy harvesting. *Int. J. RF Microw. Comput.-Aided Eng.* **2019**, *29*, e21651. [CrossRef]
52. Yoshida, S.; Fukuda, G.; Kobayashi, Y.; Tashiro, S.; Noji, T.; Nishikawa, K.; Kawasaki, S. The C-band MPT rectifier using a HEMT without bonding-wire connection for a space health monitoring system. In Proceedings of the 2013 IEEE Wireless Power Transfer (WPT), Perugia, Italy, 15–16 May 2013; pp. 163–166.

53. Bougas, I.D.; Papadopoulou, M.S.; Boursianis, A.D.; Kokkinidis, K.; Goudos, S.K. State-of-the-Art Techniques in RF Energy Harvesting Circuits. *Telecom* **2021**, *2*, 369–389. [[CrossRef](#)]
54. Papadopoulou, M.S.; Boursianis, A.D.; Skoufa, A.; Volos, C.K.; Stouboulos, I.N.; Nikolaidis, S.; Goudos, S.K. Dual-Band RF-to-DC Rectifier with High Efficiency for RF Energy Harvesting Applications. In Proceedings of the 2020 9th International Conference on Modern Circuits and Systems Technologies (MOCASST), Bremen, Germany, 7–9 September 2020; pp. 1–4. [[CrossRef](#)]
55. RT/duroid®5870/5880: High Frequency Laminates. Available online: <https://rogerscorp.com/-/media/project/rogerscorp/documents/advanced-electronics-solutions/english/data-sheets/rt-duroid-5870---5880-data-sheet.pdf> (accessed on 14 September 2022).
56. Bougas, I.D.; Papadopoulou, M.S.; Psannis, K.; Sarigiannidis, P.; Goudos, S.K. State-of-the-Art Technologies in RF Energy Harvesting Circuits – A Review. In Proceedings of the 2020 3rd World Symposium on Communication Engineering (WSCE), Thessaloniki, Greece, 9–11 October 2020; pp. 18–22. [[CrossRef](#)]
57. Ohira, T. Power efficiency and optimum load formulas on RF rectifiers featuring flow-angle equations. *IEICE Electron. Express* **2013**, *10*, 20130230. [[CrossRef](#)]
58. HSMS-286x Series: Surface Mount Microwave Schottky Detector Diodes. Available online: https://gr.mouser.com/datasheet/2/678/V02_1388EN0-1222339.pdf (accessed on 14 September 2022).
59. AN5457: RF Matching Network Design Guide for STM32WL Series. Available online: https://www.st.com/resource/en/application_note/an5457-rf-matching-network-design-guide-for-stm32wl-series-stmicroelectronics.pdf (accessed on 14 September 2022).
60. Zeng, M.; Andrenko, A.S.; Liu, X.; Zhu, B.; Li, Z.; Tan, H.Z. Differential topology rectifier design for ambient wireless energy harvesting. In Proceedings of the 2016 IEEE International Conference on RFID Technology and Applications (RFID-TA), Shunde, China, 21–23 September 2016; pp. 97–101.

Disclaimer/Publisher’s Note: The statements, opinions and data contained in all publications are solely those of the individual author(s) and contributor(s) and not of MDPI and/or the editor(s). MDPI and/or the editor(s) disclaim responsibility for any injury to people or property resulting from any ideas, methods, instructions or products referred to in the content.